JGR Biogeosciences

RESEARCH ARTICLE
10.1029/2026JG009783

Exorcizing Divergence in Tree-Ring Density Along the Rocky Mountains

Marcel Kunz[1], Max C. A. Torbenson[2,3], Frederick Reinig[1], Edurne Martinez del Castillo[1], Ulf Büntgen[3,4,5], Rob Wilson[6,7], Inga K. Homfeld[1], Greg King[8], Emily Reid[6], Kevin J. Anchukaitis[7,9,10], Valerie Trouet[9,10], Karen E. King[11], Grant L. Harley[12], Justin T. Maxwell[13], Adam Csank[14], Ellie Broadman[10], Eileen Kuhl[15], Julie Edwards[16], Philipp Römer[1], Björn Günther[17,18], Christian Gerber[18,19], and Jan Esper[1,3]

[1]Department of Geography, Johannes Gutenberg University, Mainz, Germany, [2]Department of Geography, Texas A&M University, College Station, TX, USA, [3]Global Change Research Institute of the Czech Academy of Sciences (CzechGlobe), Brno, Czech Republic, [4]Department of Geography, University of Cambridge, Cambridge, UK, [5]Department of Geography, Faculty of Science, Masaryk University, Brno, Czech Republic, [6]School of Earth and Environmental Sciences, University of St. Andrews, St. Andrews, UK, [7]Tree Ring Laboratory, Lamont-Doherty Earth Observatory, Palisades, NY, USA, [8]Department of Science, University of Alberta Augustana Campus, Camrose, AB, Canada, [9]School of Geography, Development, and Environment, University of Arizona, Tucson, AZ, USA, [10]Laboratory of Tree-Ring Research, University of Arizona, Tucson, AZ, USA, [11]Department of Geography and Sustainability, University of Tennessee, Knoxville, TN, USA, [12]Department of Earth and Spatial Sciences, University of Idaho, Moscow, ID, USA, [13]Department of Geography, Indiana University Bloomington, Bloomington, IN, USA, [14]Department of Geography, University of Nevada, Reno, Reno, NV, USA, [15]Deutscher Wetterdienst (German Meteorological Service), Offenbach, Germany, [16]Bren School of Environmental Science & Management, Santa Barbara, CA, USA, [17]Chair of Soil Resources and Land Use, Institute of Soil Science and Site Ecology, Dresden University of Technology, Tharandt, Germany, [18]Core Facility Environmental Analytics (CFEA), Dresden University of Technology, Tharandt, Germany, [19]Chair of Forest Utilization, Institute of Forest Utilization and Technology, Dresden University of Technology, Tharandt, Germany

Abstract Briffa et al. (1998), https://doi.org/10.1038/35596 published a seminal paper on the reduced sensitivity of annual tree growth to temperature across Northern Hemisphere treeline stands. By averaging tree-ring chronologies to sub-continental means, they found decade-long trends in maximum latewood density (MXD) progressively diverging from observed warming temperatures since the 1960s. This divergence challenges the reliability of the proxy, but the lack of an intercontinental network of up-to-date MXD chronologies extending into the 21st century hindered large-scale evaluations of the phenomenon, leaving it unresolved. Here, we introduce nine new MXD chronologies along the North American Rocky Mountains between 38° and 69°N and analyze their trends after applying novel approaches to preserve low-frequency variability. When following the original Briffa et al. (1998), https://doi.org/10.1038/35596 methodology, the divergence between increasing temperatures and MXD chronologies reaches offset values greater than 1°C by 2020 CE. However, divergence markedly decreases and even disappears entirely when MXD chronologies are (a) based on high-replication data sets including differently old trees, (b) detrended using signal-free age-dependent splines instead of Hugershoff curves, and (c) calibrated against optimum season instead of April–September temperatures. MXD chronologies north of 60°N exhibit stable relationships with regional summer temperatures on interannual to multi-decadal timescales, but at the southern sites, a lack of high-frequency proxy-target coherency is evident starting in the second half of the 20th century. This study emphasizes the importance of careful site and target selection, sampling design, and chronology development for overcoming the divergence problem and reconstructing summer temperatures from MXD data in North America.

Plain Language Summary Trees growing in cold regions of the Northern Hemisphere often produce denser wood during warm summers. Because of this, wood density from such locations can be used to estimate past climate conditions. However, previous research has found that many of these tree-ring records do not reflect the strong warming trend observed in recent decades. This problem, known as "divergence," questions how reliable tree rings are for reconstructing past climate. Here, we present new wood density data from nine locations along the Rocky Mountains in western North America. We demonstrate that divergence in these sites can be minimized by using a large number of trees of different ages, applying suitable techniques for analysis, and selecting the part of the year that most strongly affects tree growth at each site. Our results show that the link

Key Points:

- Tree-ring density continues to track recent warming trends in Western North America
- Divergence between proxy and instrumental data is minimized by thorough site and target selection and suitable methodology
- Interannual variations in tree growth in the southern Rocky Mountains are increasingly determined by water availability

Supporting Information:

Supporting Information may be found in the online version of this article.

Correspondence to:

M. Kunz,
mkunz01@uni-mainz.de

Citation:

Kunz, M., Torbenson, M. C. A., Reinig, F., Martinez del Castillo, E., Büntgen, U., Wilson, R., et al. (2026). Exorcizing divergence in tree-ring density along the Rocky Mountains. *Journal of Geophysical Research: Biogeosciences*, *131*, e2026JG009783. https://doi.org/10.1029/2026JG009783

Received 6 FEB 2026
Accepted 8 MAY 2026

Author Contributions:

Conceptualization: Marcel Kunz, Max C. A. Torbenson, Frederick Reinig, Edurne Martinez del Castillo, Jan Esper
Data curation: Marcel Kunz, Björn Günther, Christian Gerber
Formal analysis: Marcel Kunz, Jan Esper
Funding acquisition: Ulf Büntgen, Jan Esper
Investigation: Marcel Kunz, Jan Esper
Methodology: Marcel Kunz, Max C. A. Torbenson, Frederick Reinig, Edurne Martinez del Castillo, Jan Esper
Project administration: Jan Esper
Supervision: Max C. A. Torbenson, Jan Esper
Visualization: Marcel Kunz, Frederick Reinig, Jan Esper

Writing – original draft: Marcel Kunz
Writing – review & editing: Max C. A. Torbenson, Frederick Reinig, Edurne Martinez del Castillo, Ulf Büntgen, Rob Wilson, Inga K. Homfeld, Greg King, Emily Reid, Kevin J. Anchukaitis, Valerie Trouet, Karen E. King, Grant L. Harley, Justin T. Maxwell, Adam Csank, Ellie Broadman, Eileen Kuhl, Julie Edwards, Philipp Römer, Jan Esper

between instrumental temperatures and tree-ring data has remained stable in the northern half of our study area across both short and long periods. In contrast, in the southern Rocky Mountains, changes in tree growth from year to year are increasingly influenced by dry conditions rather than temperature.

1. Introduction

The divergence problem (D'Arrigo et al., 2008), describing an offset between instrumental temperature measurements and tree-ring proxy data since the mid-20th century, remains a significant issue in paleoclimatology (Büntgen, Allen, et al., 2021). Such non-stationary responses to climate forcing can be characterized by either a temporal shift in trend or interannual coherence, two phenomena that may occur simultaneously and contribute to each other (Esper & Frank, 2009). Briffa et al. (1998) identified divergence as becoming increasingly prevalent toward the end of their investigated period in the 1980s, primarily in terms of trend rather than interannual correlation between the proxy and the instrumental target. They showed that smoothed tree-ring width (TRW) and maximum latewood density (MXD) mean chronologies underestimated instrumentally measured temperatures by more than 1 and, in some cases, even 2 standard deviations when averaged over larger regions. These observations questioned both the reliability of proxy-based temperature reconstructions and the extent to which forests could act as carbon sinks in a warming world. Since then, a variety of studies, primarily based on TRW, have addressed regional expressions of divergence and potential explanations such as increasing drought stress (Barber et al., 2000; D'Arrigo et al., 2009; Kirdyanov et al., 2025; Porter & Pisaric, 2011; Wang et al., 2017), thermal thresholds (D'Arrigo et al., 2004; Vaganov et al., 2011), target temperature limitations (Esper et al., 2010), "global" (Stanhill & Cohen, 2001; Wild, 2009) or "Arctic dimming" (Büntgen, Kirdyanov, et al., 2021; Kirdyanov et al., 2020; Stine & Huybers, 2014) caused by anthropogenic aerosols, stand dynamics (Grudd, 2008), and methodological issues (Büntgen et al., 2008, 2011; Esper et al., 2005; Frank et al., 2007; Loehle, 2009). MXD, as well as latewood and delta blue intensity as its less expensive surrogates (Björklund et al., 2024; R. Campbell et al., 2007; Wilson et al., 2019), are often considered superior proxies for tree-ring based temperature reconstructions (De Mil et al., 2024; Esper et al., 2018; Klippel et al., 2020; Reid et al., 2025) due to weaker inherent autocorrelation and memory effects compared to TRW (Esper et al., 2015). Although blue intensity measures similar wood properties to MXD (Wilson et al., 2019) and has increasingly been used for regional temperature reconstructions (Fuentes et al., 2018; Harley et al., 2021; Heeter et al., 2021), its potential limitations include discoloration issues, color differences between heartwood and sapwood as well as measurement resolution (Björklund et al., 2024; Rydval et al., 2014; Seftigen et al., 2022). An update based on MXD data as the state-of-the-art proxy has been largely missing on a continental scale.

In their original study, Briffa et al. (1998) compiled 314 single sites at high latitude or elevation across the Northern Hemisphere, 83 of which are located in North America, from which typically 24 to 30 samples (from 12 to 15 trees) were taken. They detrended the TRW and MXD data using the "Hugershoff" method, which is a combination of polynomial and exponential functions (Hugershoff, 1936). They derived site chronologies by calculating simple arithmetic means of the detrended single series and subsequently combined these into eight large regional means. Subtracting instrumental temperature from tree-ring (TR) data, after scaling these to equal mean and standard deviation, revealed greater trend divergence in northern than in southern regions with the most significant offset in Siberia. Divergence was less pronounced but still evident in Western North America (WNA) (Briffa et al., 1992). With all MXD series used in their paper ending in 1983, the most recent 40 years of accelerated warming across the region (Booth et al., 2012; IPCC, 2023) along with an increased frequency of heatwaves (Perkins-Kirkpatrick & Lewis, 2020) were not part of their analysis.

Here, we present an updated assessment of divergence along the Rocky Mountains, the major longitudinal mountain chain in WNA, by resampling through the domain of the original Briffa et al. (1998) network that outlined an offset in trend with instrumental records (Figure 1). Our nine new MXD chronologies span 147–460 years, including the crucial 40-year period of rapid warming since the 1980s. We compare our results with those of Briffa et al. (1998) and examine the influence of larger replication and a more diverse age structure of our samples. We test how different detrending methods as well as target temperatures and seasons affect divergence-like effects. Finally, we combine our single sites into a northern and southern composite to emphasize larger-scale covariance structures and different characteristics.

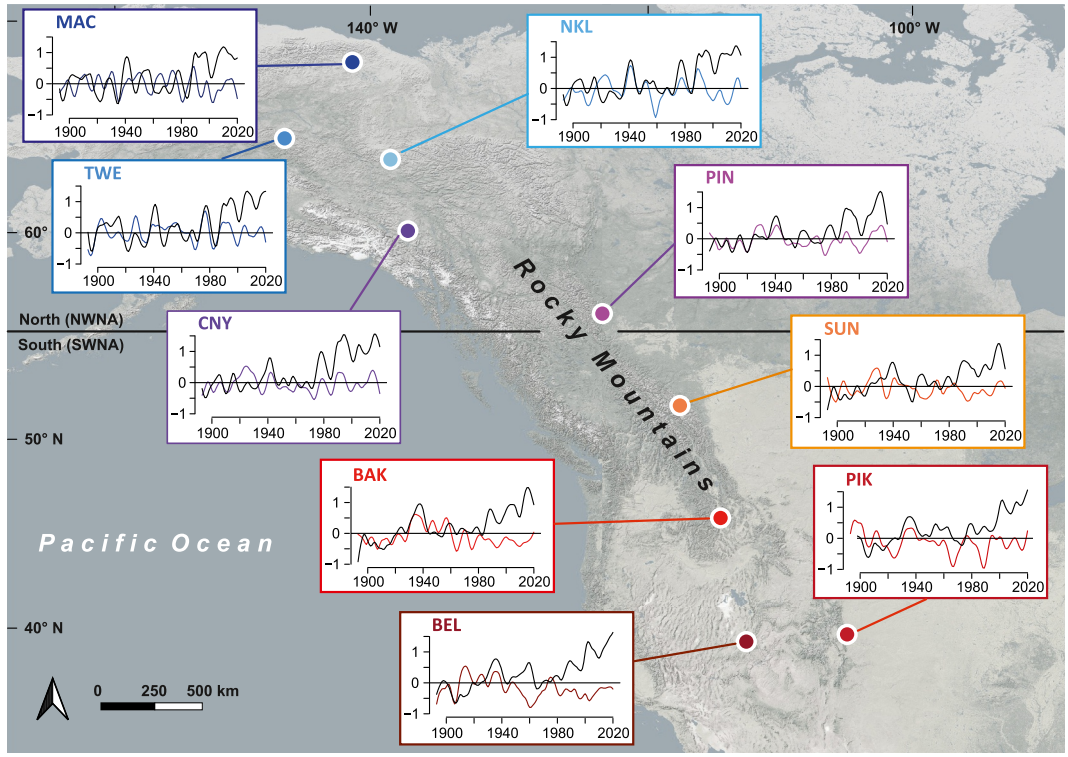

Figure 1. Divergence at nine tree-ring sites along the Rocky Mountains. Horizontal black line indicates the boundary between the North-West (NWNA) and South-West North American (SWNA) regions according to Briffa et al. (1998). Diagrams show 10-year smoothed April–September temperature anomalies in °C (black; Rohde & Hausfather, 2020) and scaled MXD data (colored curves) on *y*-axes.

2. Material and Methods

2.1. Sampling and Site Description

Samples were collected during several field campaigns in the summers of 2022 and 2023 within the context of a larger sampling effort for the Monostar project, which aims to assess and explain divergence across the Northern hemisphere (CORDIS | European Commission, n.d.). The nine sites (Figure 1, Table 1, and Figure S1 in Supporting Information S1) are distributed throughout the entire length of the Rocky Mountains. Five sites form a northern group (Mancha Creek (MAC), Twelvemile Summit (TWE), North Klondike River (NKL), Canyon Lake (CNY), Pink Mountain (PIN)) while the southern group consists of four sites, Sunwapta (SUN), Baker Lake (BAK), Pikes Peak (PIK), and Mount Belknap (BEL). Site selection aimed to represent near-treeline conditions with elevations ranging from 566 m a.s.l. at the northernmost site (MAC) and 3583 m at the southern PIK site, reflecting the altitudinal increase of the treeline with decreasing latitude. At each location, at least 50 living trees were sampled: white spruce (*Picea glauca* [Moench] Voss.) at the five northern sites and Engelmann spruce (*Picea engelmannii,* Parry ex. Engelmann) at the four southern sites. In deviation from common dendroclimatological approaches, efforts were made to sample trees of mixed ages, including relatively young individuals of less than 50 years.

The separation between the northern and southern regions not only reflects the boundary between the North-West (NWNA) and South-West North American (SWNA) regions in Briffa et al. (1998) but also the boundary between the boreal forests of the north and temperate climate conditions in the south (Frelich, 2020). Average climate patterns vary greatly among the sites with large differences between winter and summer temperatures in the north and smaller amplitudes in the south (Table 1). The increase in annual mean temperature since 1981 ranges from 0.20°C (CNY, SUN) to 0.33°C (TWE) per decade (Rohde & Hausfather, 2020). The highest amounts of annual precipitation are measured in the southern half of the transect (Table 1), albeit with large differences in seasonal distribution (Daly et al., 1994; Harris et al., 2020), for example, a typical dry spell in early summer before the

Table 1
Sampling Site Characteristics

Site	Mancha Creek	Twelvemile Summit	North Klondike River	Canyon Lake	Pink Mountain	Sunwapta	Baker Lake	Pikes Peak	Mount Belknap
Code	MAC	TWE	NKL	CNY	PIN	SUN	BAK	PIK	BEL
Latitude	68.67	65.38	64.44	61.12	57.04	52.21	45.89	38.87	38.42
Longitude	−141.02	−145.95	−138.26	−136.99	−122.86	−117.22	−114.27	−105.07	−112.40
Elevation [m a.s.l.]	566	971	984	1108	1512	2051	2423	3583	3179
Summer T_{mean} [°C]	−2	6	6	6	9	4	10	5	8
Winter T_{mean} [°C]	−24	−19	−21	−14	−9	−9	−3	−7	−4
Summer Prec [mm]	80–140	140–200	190–250	110–170	305–350	435–495	340–4000	450–500	410–470
Winter Prec [mm]	5–65	15–75	100–160	30–80	165–225	685–720	580–640	160–220	740–800
May-July Prec [mm]	45–75	950–125	105–135	75–105	190–220	230–260	170–200	225–255	130–160
Period	1794–2021	1612–2021	1795–2021	1820–2021	1864–2022	1480–2021	1460–2020	1539–2021	1560–2021
Period n ≥ 5	1808–2021	1873–2021	1823–2021	1835–2021	1874–2022	1561–2021	1727–2020	1567–2021	1607–2021
Replication	100	99	100	100	100	99	96	113	93
MSL	117	73	118	120	115	169	177	140	175
AR1	0.22	0.00	0.27	0.23	0.13	0.30	0.36	0.36	0.48
Rbar	0.3	0.42	0.22	0.29	0.38	0.21	0.17	0.23	0.09
Year EPS ≥0.85	1868	1891	1886	1870	1894	1796	1766	1699	1850

Note. Climate data refer to nearest including coordinates, elevation, mean temperature and precipitation estimates for summer (April–September) and winter (October–March) half-years and May–July (1961–90) based on single month estimates according to nearest CRU TS 4.08 grid cells (Harris et al., 2020) in Alaska and Canada and nearest PRISM grid cell (Daly et al., 1994) in the contiguous US. MSL is mean segment length, AR1 is first-order autocorrelation, Rbar is interseries correlation, and EPS the Expressed Population Signal (Wigley et al., 1984).

onset of monsoonal rainfall at the southernmost BEL site (Birch et al., 2024) and drier winters at the eastern PIK site. Effects of different sampling strategies and tree replication on climate-growth relationships were assessed by comparing trends and correlation statistics of Briffa et al.'s (1998) nearest sampling sites to our locations. Their northern sites were at lower elevations than in this study, but locations and elevations were more similar in the south (Table S1 in Supporting Information S1).

2.2. Data Composition and Treatment

After measuring TRW reference data using LINTAB 6 devices (Rinntech, Germany) and TSAP software (Rinn, 2003) to later facilitate MXD crossdating, samples were cut into 1.2 mm thin sections orthogonal to the tracheids' longitudinal axis to account for changes in fiber angle. After X-raying, the brightness of the resulting images was recorded at a resolution of 0.01 mm using a DENDRO2003 X-ray microdensitometer (WALESCH Electronic GmbH, Switzerland) as described in Björklund et al. (2019) and the resulting MXD values were extracted. Crossdating of all measurements was validated using COFECHA (Holmes, 1983) software. To compare the updated MXD data with those from Briffa et al. (1998), we selected the sites in their study that were closest to our locations (Table S1 in Supporting Information S1). For each location, we compared three MXD data sets, each of which were power-transformed and detrended using the Hugershoff function (Cook & Kairiukstis, 1990) in ARSTAN (Cook, 1985; Cook et al., 2017a): (a) our new full-replication MXD data sets (MonostarALL) including 93–113 series per site, (b) the respective Briffa et al. (1998) counterparts, and (c) a subset of the oldest series at each of our sites with the same replication as the corresponding Briffa sites as an attempt to reflect the conventional dendroclimatological sampling strategy (MonostarOLD). In addition, the MonostarALL data sets were detrended using the signal-free version of an age-dependent spline (Helama et al., 2017; Melvin & Briffa, 2008; Melvin et al., 2007) with an initial spline stiffness of 50 years and positive trend retention in SigFree

(Cook et al., 2017b), which has successfully been applied in research across the region (Heeter et al., 2021; Kunz et al., 2025; Leland et al., 2025; Reid et al., 2025; Wilson et al., 2019).

2.3. Divergence Assessment

For each proxy-target combination, 31-year moving Pearson correlations were calculated to assess higher-frequency changes in the relationship between MXD and monthly temperature anomalies of the 1° × 1° grid cells in the Berkeley Earth data set (Rohde et al., 2013; Rohde & Hausfather, 2020) surrounding each site. Monthly Berkeley Earth mean (T_{mean}) and maximum (T_{max}) temperature data (1893–2020) as well as precipitation and self-calibrated Palmer Drought Severity Index (PDSI) (Wells et al., 2004) data from version 4.08 of the CRU TS data set (0.5° × 0.5° grid cells) (Harris et al., 2020) were extracted from the KNMI climate explorer (Trouet & Van Oldenborgh, 2013). Additionally, the detrended MXD chronologies were scaled to the instrumental temperature series by adjusting mean and standard deviation for the period 1893–1950, which we here define as the baseline period before what is traditionally considered the divergence "problem" (Esper & Frank, 2009). Residual trends (RT) for the post-calibration period (1951–2020) were calculated by multiplying the length of the period in years by the slopes of linear regressions of 10-year low-pass filtered residual chronologies between scaled MXD and temperature timeseries to quantify trend differences. To initially compare with the Briffa et al. (1998) sites, the period was split into two parts (1951–1983 and 1984–2020). For the same periods, root mean squared errors (RMSE) of these smoothed residuals between the proxy and target were computed, serving as a combined measure of trend and higher-frequency coherence. Divergence was assessed using instrumental temperature data of the April–September seasonal average (Briffa et al., 1992, 1998) as well as individual optimum single months or seasons for each site, which were determined using static (1894–2020) correlations of first-differenced temperature and MXD timeseries. Analyses were conducted using R version 4.5.1. (R Core Team, 2024) as well as the "dplR" (Bunn, 2008), "treeclim" (Zang & Biondi, 2015), and "dendroTools" (Jevšenak & Levanič, 2018) R packages and correlation maps were produced using the KNMI climate explorer (Trouet & Van Oldenborgh, 2013).

3. Results

3.1. Chronology Characteristics and Comparison With Briffa et al. Sites

Our five northern sites are notably younger (each reaching a replication of five samples only during the 19th century) than the four southern ones, for which the initial dates vary between 1561 (SUN) and 1727 (BAK) (Table 1). Similarly, the mean sample length is shortest in TWE in Alaska (73 years) and longest in BAK in Montana (177 years). First-order autocorrelation of the detrended MXD chronologies was significantly higher in the south (0.30–0.48) than in the north (0.00–0.27), likely reflecting the age difference between the two groups. Mean interseries correlation (Rbar) is typically higher in the north (0.22–0.42 vs. 0.09–0.23) and the EPS of all site chronologies exceeds the commonly utilized value of 0.85 (Wigley et al., 1984) by 1894 at the latest (Figure S2 in Supporting Information S1), indicating sufficient quality over the common period with instrumental data.

Moving correlations with April–September mean temperatures, the target used in Briffa et al. (1998), reveal slightly higher values for MonostarALL compared to MonostarOLD (Figures 2a and 2c) but overall similar patterns and periods of significance. For the southern part of the transect, the correlation mean and correlations for all sites (Figure S3 in Supporting Information S1) decrease toward the end of the 20th century and become temporarily insignificant ($p < 0.05$). Also, correlations across the full period (1893–2020) are higher for MonostarALL on average and for most single sites with the largest difference for MAC and SUN (Figure S4 in Supporting Information S1). However, the decrease in correlation at BEL is even stronger when using all samples instead of the old subset. Results for the Briffa et al. sites differ between the northern and the southern groups. Their MXD chronologies consistently show weaker correlations to April–September mean temperatures in the north, and similar correlations as the Monostar data sets in the south during the common period of all data sets (1893–1983). Residual trends within the two regions (Figures 2b and 2d) are similar among MonostarALL and MonostarOLD with increasingly negative residuals from the 1970s onwards. RT differences between the Monostar data sets are minor before the end of the Briffa chronologies in 1983 and RT is more negative for MonostarOLD in the north (−0.97 vs. −0.86) and less negative in the south (−0.66 vs. −0.74) for the subsequent period (1984–2020). The RMSE of MonostarALL is lower for the north than the south (0.32 and 0.94 vs. 0.40 and 1.05) and all values are slightly lower than the respective results with MonostarOLD for both periods. From 1951

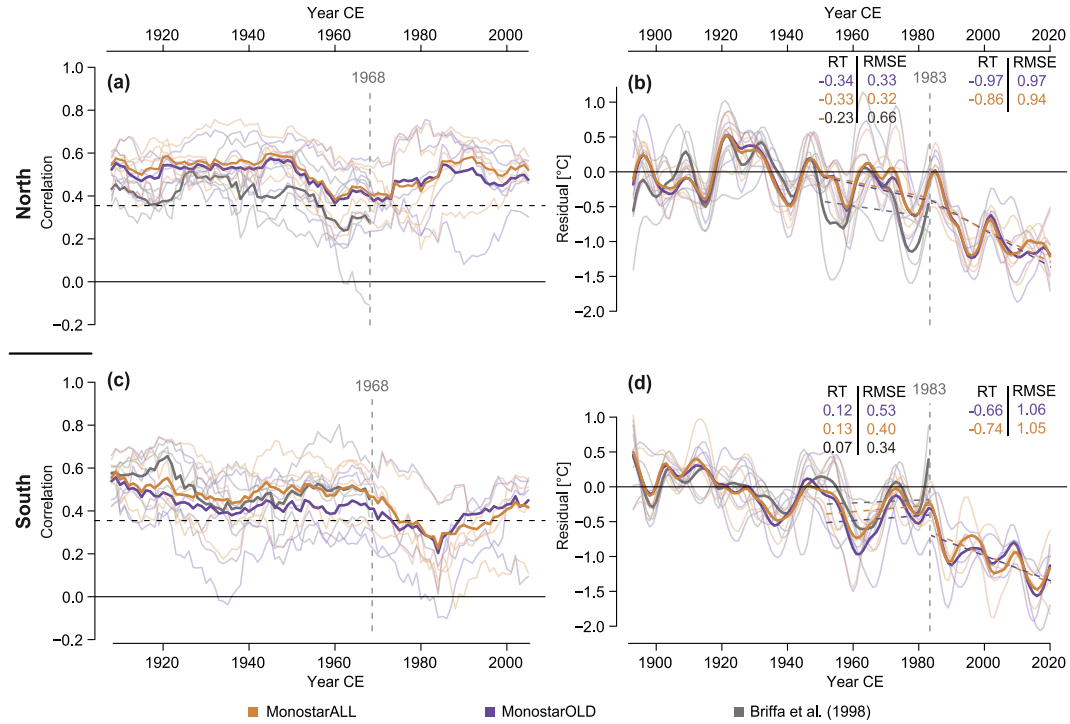

Figure 2. Centered 31-year moving correlations (a, c) and 10-year smoothed residual trends (b, d) between regional April–September mean temperatures and Hugershoff detrended MonostarALL, MonostarOLD, and Briffa et al. (1998) chronologies. All chronologies were scaled from 1893 to 1950. Thin lines refer to single sites and solid lines to group means. RMSE and linear residual trends (RT) in °C are calculated over the 1951–1983 common period and the 1984–2020 recent period (dashed lines in panels b and d). Vertical dashed lines indicate the final years covered by the Briffa et al. (1998) sites.

to 1983, the Briffa et al. (1998) residuals decline more strongly in the north with a substantially higher RMSE than MonostarALL and OLD (0.66 vs. 0.32 and 0.33), while showing a sharp increase toward the end in the south. Overall, the strongest results regarding highest correlation strength and stability, weakest RT, as well as lowest RMSE are achieved with MonostarALL, which is therefore used for further analysis.

3.2. Selecting Optimal Temperature Parameters and Detrending Versions

Moving correlations between MXD chronologies and instrumental temperatures are slightly higher for T_{max} than T_{mean} in both the north and south (Figures S5a and S5c in Supporting Information S1). The gap between T_{max} and T_{mean} correlations is overall larger in the first half of the 20th century, especially for NKL, CNY, and PIK (Figure S6 in Supporting Information S1). RMSE values are lower for T_{max} than T_{mean} in both regions (0.70 vs. 0.72 in the north, 0.74 vs. 0.81 in the south) (Figures S5b and S5d in Supporting Information S1), highlighting T_{max} as the more suitable calibration target for higher-frequency variability. To exclude potential biases due to gridded data set selection, the results were additionally calculated for CRU TS temperatures (Figure S7 in Supporting Information S1), indicating notably stronger moving correlations for Berkeley Earth in the north and very similar results in the south.

Utilizing signal-free age-dependent spline detrending (SF ADS) (Melvin & Briffa, 2008) instead of Hugershoff functions (Figure 3) leads to only slightly stronger moving correlations but strongly improves both RT (−0.9 vs. −1.49 in the north, −0.38 vs. −1.14 in the south) and RMSE values (0.41 vs. 0.70 and 0.37 vs. 0.74, respectively) by increasing consistency between the trends of MXD and target T_{max}. Single sites (Figure S8 in Supporting Information S1) demonstrate a similar shift in trend and again only marginal improvement in interannual coherence. CNY, SUN, and BEL show the greatest improvement in terms of trend and CNY, BAK, and BEL in terms of RMSE.

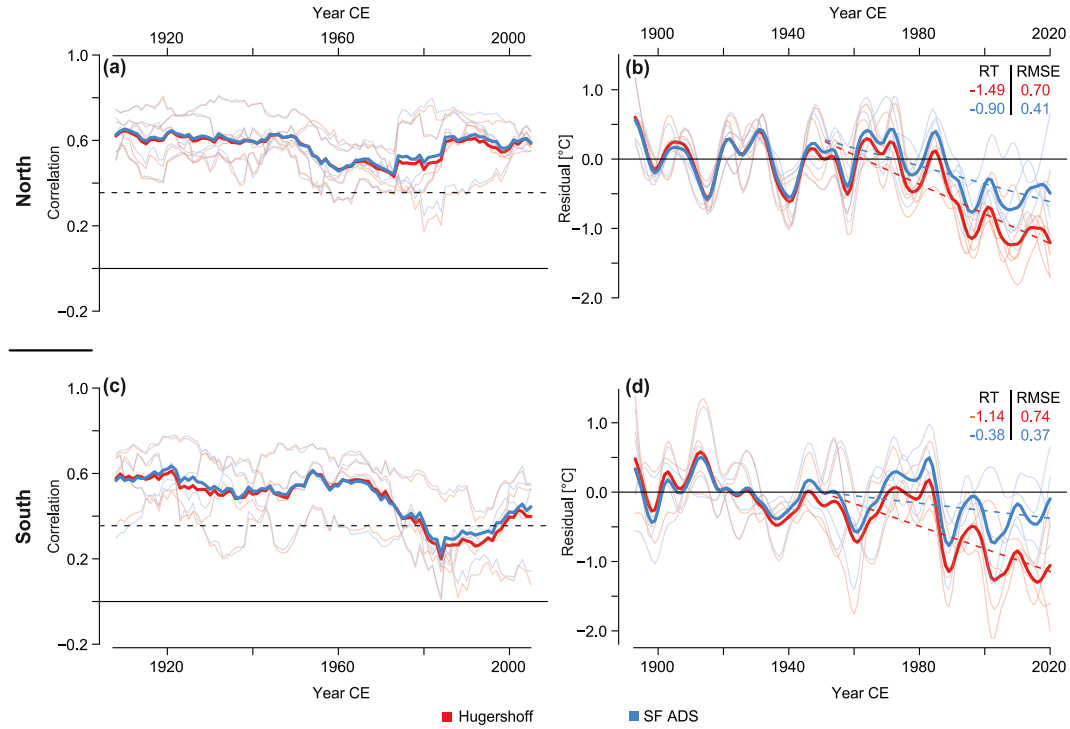

Figure 3. Centered 31-year moving correlations (a, c) and trends of 10-year smoothed residuals (b, d) calculated between regional April–September maximum temperatures and Hugershoff or signal-free age-dependent spline (SF ADS) detrended MXD chronologies. All chronologies were scaled from 1893 to 1950. Thin lines refer to single sites and solid lines to group means. RMSE and linear residual trends (RT) in °C are calculated over the 1951–2020 period.

3.3. Variations in Optimal Target Seasons

To test the effect of varying seasonality on divergence, first-difference detrended T_{max} and MXD timeseries were correlated for various combinations of current year spring and summer months across the whole period (1894–2020; Figure 4). Correlations were strongest for May–August for the three northernmost sites and BAK, July–August for CNY, PIN, and SUN, and August only for PIK and BEL. These optimum season correlations are highly significant for all sites ($p < 0.001$) and range from 0.64 (BEL) to 0.76 (SUN). Correlations for the original April–September season ranged from 0.40 (BEL) to 0.67 (NKL) and differences between April and September and optimum seasons were larger for the northern and southern ends of the transect than for intermediate sites. Mean correlations across all sites are slightly higher for first-differenced compared to non-transformed versions and are highest for the May–August season (Figure 4j).

Applying site-specific optimum seasonal windows enhances coherence for regional averages (Figures 5a and 5c) and all single sites (Figures S4 and S9 in Supporting Information S1) and yields continuous significant ($p < 0.05$) mean moving correlations also for the southern part of the transect (Figure 5c) where the April–September version temporarily declined and became non-significant toward the end of the 20th century. Choosing individual windows for each site compared to the Briffa et al. (1998) April–September season also eliminates a large part of the residual trend between MXD and target temperatures. Specifically, RT values become less negative, changing from −0.90 to −0.33 in the north and from −0.38 to −0.12 in the south (Figures 5b and 5d). Compared to the fixed April–September window, the RMSEs are further minimized and limited to 0.25 in the north and 0.36 in the south when optimum season temperatures are applied.

3.4. Regional Composites and Drought Impacts

Combining the five northern sites into a single regional data set and correlating and scaling it against larger-scale regional temperature data further enhances interannual coherence. Correlations are highly significant ($p < 0.001$) across the entire region from Central Alaska to Northern British Columbia (Figure 6c) with May–August as the strongest target season ($r = 0.76$; Figure 6a). Moving correlations (Figure 6b) are continuously stronger for the

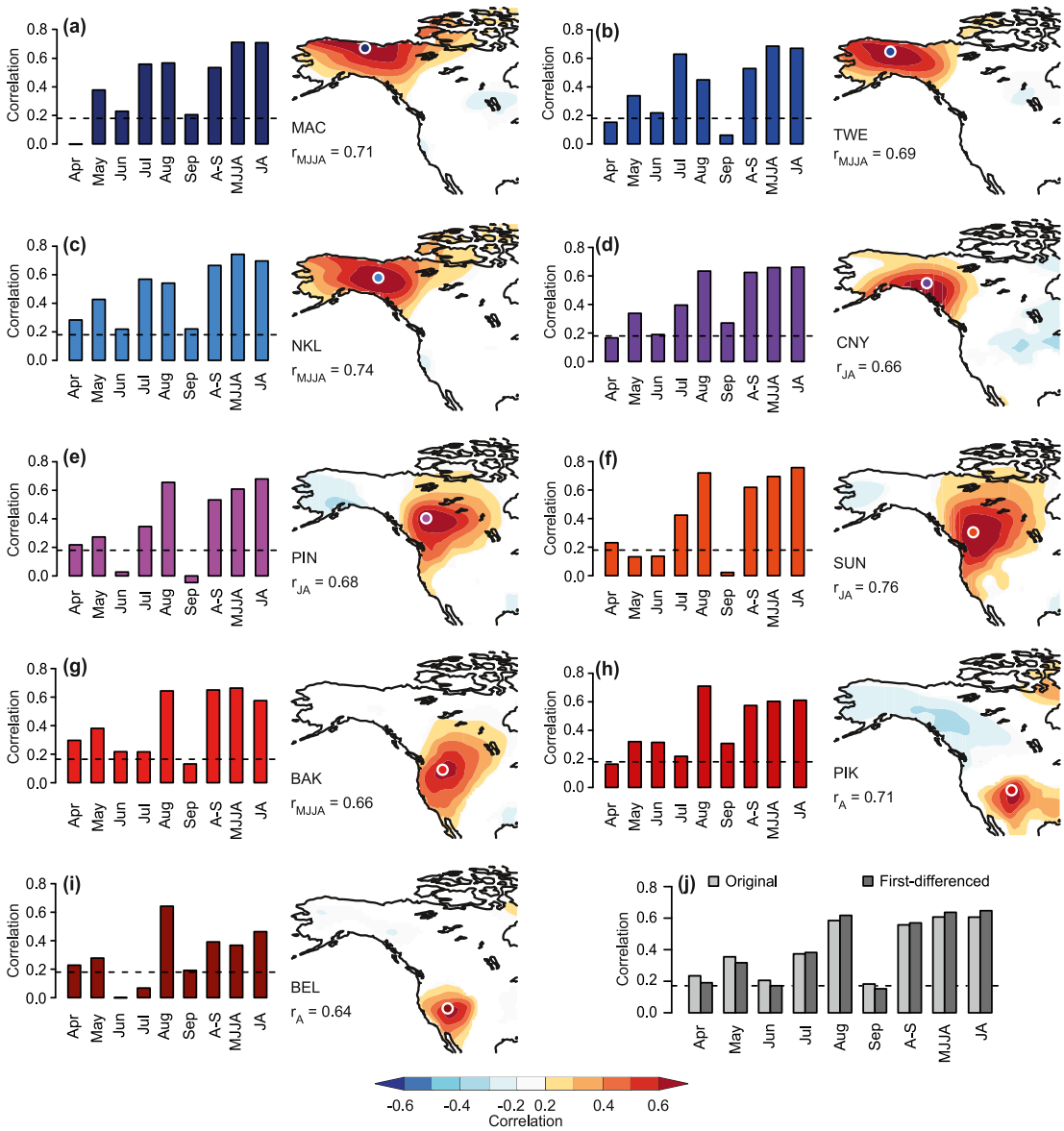

Figure 4. Correlations between first-differenced site chronologies and maximum temperatures for warm-season months and seasons from 1894 to 2020 (a–i). Maps show spatial first-differenced correlations of the strongest season for each site. (j) Mean correlations for original (light gray) and first-differenced (dark gray) data.

composite than for the simple site mean, representing the approach originally used by Briffa et al. (1998), apart from a short period during the 1970s. The regional instrumental temperatures (Figure 6e) have risen more sharply in recent decades compared to the single grid point mean (Figure 6d), but the scaled MXD composite closely tracks this warming, producing an almost horizontal residual trendline (Figure 6f; RT = −0.09). Merging the four southern sites similarly minimizes trend divergence and even creates a slightly positive residual trend (Figure 6l), indicating that temperatures derived from MXD are higher than instrumental temperatures toward the end of the investigated period. However, the composite residuals show a striking negative peak in the late 1980s, which does not exist in the site mean. Also, correlations with August T_{max} (Figure 6g) are weaker than for the site mean and April–September is the overall strongest season for the southern composite. The decline in correlation since the 1960s is also amplified in the south when using the regional composite, resulting in a non-significant ($p < 0.05$) period during the 1980s and 1990s. Single-site correlations for equally long early and late periods (1894–1957 and 1957–2020) demonstrate that this decline in the south is not the result of a shift in seasonality, but occurs rather uniformly across months and seasons (Figure S10 in Supporting Information S1).

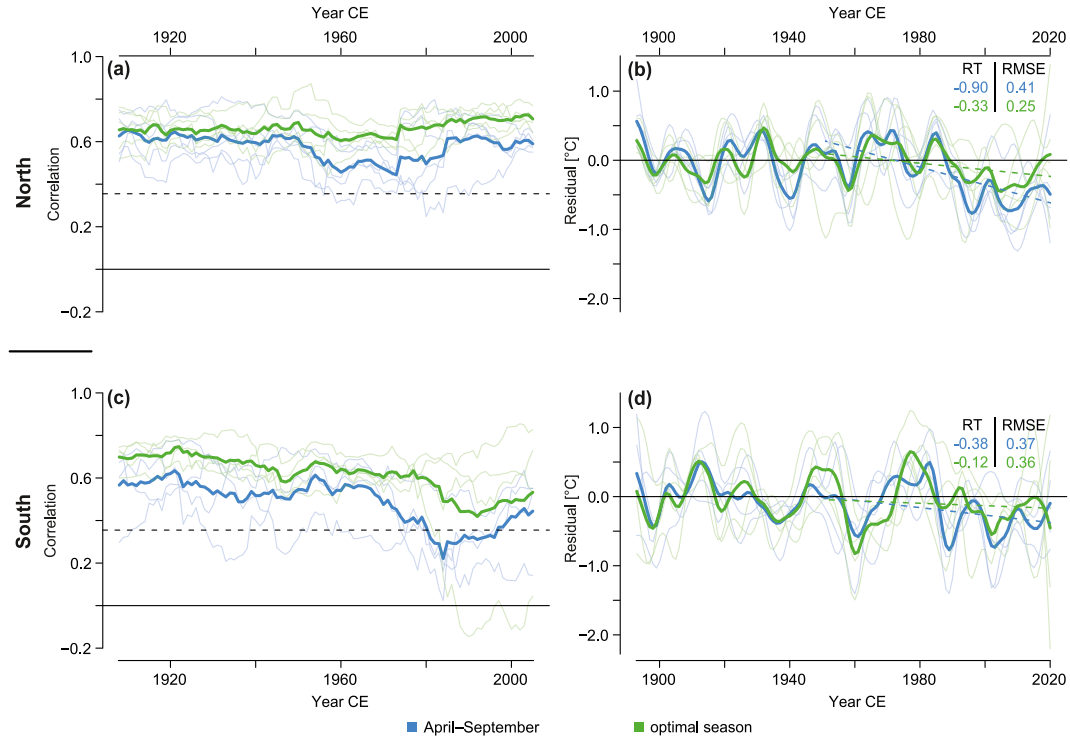

Figure 5. Centered 31-year moving correlations (a, c) and 10-year smoothed residual trends (b, d) between regional April–September and optimum season maximum temperatures and signal-free age-dependent spline detrended MXD chronologies. All chronologies were scaled from 1893 to 1950. Thin lines refer to single sites and solid lines to group means. RMSE and linear residual trends (RT) in °C are calculated over the 1951–2020 period.

Periods of reduced soil moisture may provide an explanation for this loss in sensitivity. For the southern composite, droughts around 1960 as well as in the 1980s (Trenberth et al., 1988) and 2000s (Piechota et al., 2004) correspond to large negative residuals between MXD and T_{max} (Figure 7a). Accordingly, residuals between MXD and T_{max} are strongly and increasingly correlated with regional PDSI, concurrent with declining coherence between MXD and T_{max} (Figure 7b). Spatial correlations between MXD-T_{max} residuals and PDSI sharply increased during the 1961–2020 period (Figure 7d) compared to 1901–1960 (Figure 7c) and now cover large parts of the western and central US.

4. Discussion

4.1. Effects of Data Set and Site Selection

The residual trends of the Briffa sites align surprisingly well with those of the two Monostar data sets, considering the largely different sampling locations. Potential end-effects (Sullivan et al., 2016) that occur as a sharp increase toward the southern Briffa record's final year of 1983 (Figure 2d) may arise from the applied detrending. Weaker interannual coherence with temperatures for the northern Briffa sites likely results from them being sampled at a lower elevation than the Monostar sites (Table S1 in Supporting Information S1). No climate records exist from the exact Briffa locations, but average temperatures at those northern sites are likely 1–5°C higher, considering elevational differences of 221–822 m (except for MAC, which is at similar elevation as the closest Briffa site but more than 600 km further north) and an assumed average lapse rate of 0.6°C per 100 m, and they are therefore in an environment where growth is less limited by temperature (Hartl et al., 2022; Salzer et al., 2009). In this context, these lower-elevation Briffa sites might have experienced declining temperature control under rapidly warming climate conditions of the recent decades, along with potential treeline moving upslope (Büntgen et al., 2022; Liang et al., 2026). This effect has recently been demonstrated for blue intensity data from the Yukon, where a group of high-altitude locations within a dense network of sites provided substantially stronger temperature signals than those further from treeline (Reid et al., 2025). In the south, the Briffa sites were sampled at a similar elevation as the Monostar sites, and a potential adverse effect of lower replication is masked by generally stronger

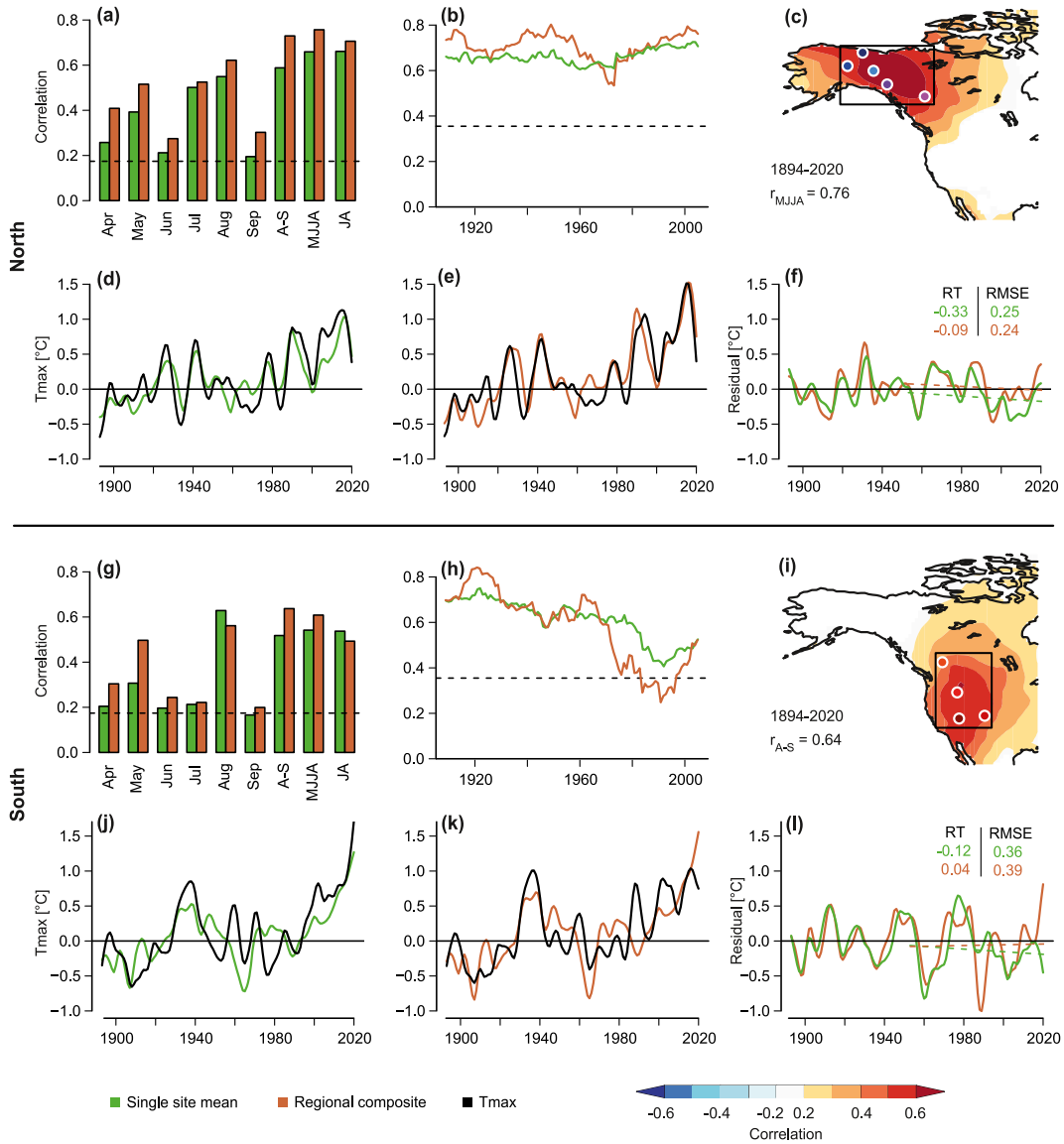

Figure 6. Correlations of the northern single sites means (green) and regional composites (brown) (1894–2020) (a). 31-year moving correlations (b) and spatial correlations (1894–2020) (c) as well as 10-year low-pass filtered, scaled (1893–1950) MXD chronologies and target temperatures (d, e) and resulting residuals (f) for the season of highest correlation. RMSE and linear residual trends (RT) in °C are calculated over the 1951–2020 period. Black borders in maps denote the grids from which instrumental temperatures were extracted. Panels (g–l) show the same data for the southern sites.

results of their Electric Lake site compared to our neighboring BEL site (Figure S3 in Supporting Information S1), despite the latter being located 200 m higher. Potential explanations might be related to slightly different microclimates, slope gradients and aspects, or soil depths (Fritts, 1976; Klesse et al., 2018; Stage, 1976) limiting the temperature response of tree growth at BEL during warm summers. However, this cannot be stated conclusively because the coordinates of Electric Lake documented in the International Tree-Ring Databank (ITRDB) might be inaccurate and do not match the recorded elevation.

Overall slightly stronger correlations with temperature for moving windows (Figures 2a and 2c) and the complete period (Figure S4 in Supporting Information S1) as well as lower RMSE (Figures 2b and 2d) for MonostarALL compared to MonostarOLD suggest beneficial effects of increasing sample replication, possibly related to using trees of different sizes and age classes. The "classic" sampling approach focusing on a limited subset of oldest trees (Nehrbass-Ahles et al., 2014) may lead to a subset that is not representative of the entire population,

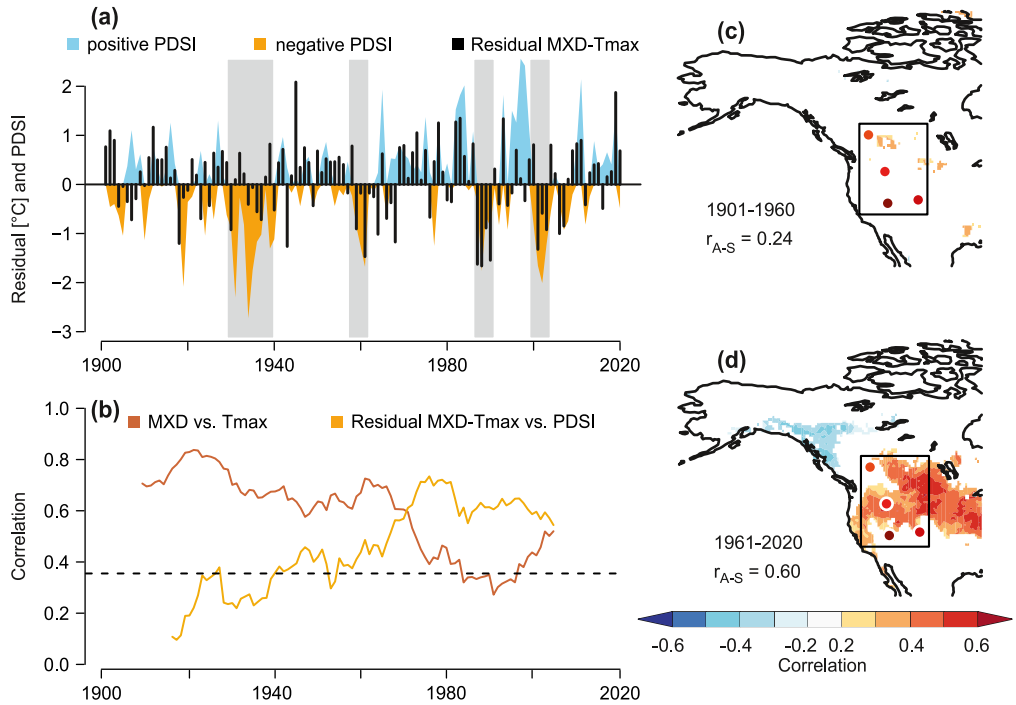

Figure 7. Effect of droughts on MXD temperature signals of the southern composite with MXD-T_{max} residuals (black bars), regional PDSI (colored areas) and major droughts of the last 120 years (gray rectangles) (a), 31-year moving correlations (centered) between MXD and T_{max} as well as between MXD-T_{max} residuals and PDSI (b) and spatial correlations (colors according to horizontal bar) between MXD-T_{max} residuals and PDSI for the 1901–1960 (c) and 1961–2020 periods (d) with black borders in maps denoting the grid from which instrumental temperatures and PDSI were extracted.

potentially introducing biases when analyzing climate-growth relationships (Bowman et al., 2013). However, including a large number of young samples, TWE being the most notable example in our transect (Figure S2 in Supporting Information S1), also increases the risk of removing part of the warming-induced positive trend by introducing or amplifying the segment-length curse (Cook et al., 1995). Although our RT results are ambiguous between MonostarALL and MonostarOLD and show no direct evidence of this effect (Figures 2b and 2d and Figure S3 in Supporting Information S1), we acknowledge a potential tradeoff between incorporating trees of all ages and optimally capturing the recent warming trend, the extent of which is also dependent on the applied detrending method.

4.2. Effects of Instrumental Target and Detrending Method Selection

While Briffa et al. (1998) used T_{mean} as their calibration target, several more recent studies across WNA (King et al., 2024; Seftigen et al., 2022; Wilson et al., 2014; Wilson & Luckman, 2003) showed that their TR data aligned better with T_{max}, both interannually and in terms of trend. These observations are confirmed by stronger T_{max} correlations with our MXD data for both parts of our transect (Figures S5a and S5c in Supporting Information S1) and all sites along the Rocky Mountains (Figures S4 and S6 in Supporting Information S1). While speculative, this pattern could be related to the stronger association of T_{max} with solar irradiation (G. G. Campbell & Vonder Haar, 1997) and its inverse relationship with cloud cover (Portmann et al., 2009), which is corroborated by independently recorded instrumental data from WNA (Figure S11 in Supporting Information S1). Light availability as an additional limiting factor (Fritts, 1976) has been suggested to be an influence at some high latitude locations, that is, in our northern group (Stine & Huybers, 2014). Stronger coherence between MXD and T_{max} than T_{mean} appears to be a persistent feature of our sites in continental WNA across both space and time. An additional impact of recent trend changes between the temperature parameters and reduced daily temperature ranges as suggested by Wilson and Luckman (2003) for southern British Columbia is not reflected in our data. Conversely, some of our individual sites (Figure S6 in Supporting Information S1) even indicate a stronger offset

in correlation of T_{mean} and T_{max} with MXD during the early and middle parts of the 20th century rather than the end.

The trends of the MXD chronologies produced by SF ADS are substantially more similar to the instrumental temperature trend than the original Hugershoff version (Figure 3 and Figure S8 in Supporting Information S1). In contrast, a weak influence of detrending method selection on coherence results is not surprising, considering the inherent trend removal when calculating moving correlations. The Hugershoff method has been widely considered suitable for density proxies due to its ability to track the typical trend of an initial increase followed by a logarithmic decline (Rydval et al., 2014; Schweingruber & Briffa, 1996). However, it evidently fails to adequately emphasize mid-frequency variation that may be linked to the recent warming. The SF ADS version applied here is more likely to avoid such a loss of warming signal in tree-ring data, provided that positive slopes of the age-dependent spline, as a data-adaptive method, are constrained. A non-increasing ADS without signal-free as available from ARSTAN produces intermediate results (Figure S12 in Supporting Information S1). The change in the detrending curve considerably enhances the fit with the instrumental temperature trend (Wilson et al., 2019) without causing an unnatural increase in amplitude compared to the earlier parts of the investigated period (McPartland et al., 2020; Pearl et al., 2017). While simply adjusting the standardization method does not completely "solve" the issue of divergence, detrending effects represent a crucial factor in the assessment of trend offsets.

4.3. Effects of Target Season Selection

The optimal seasons for dendroclimatic calibration vary significantly among regions and tree species (Hwangbo et al., 2025; Wilson et al., 2016). A comparatively long period (April–September) was used by Briffa et al. (1998) to include two distinct response peaks in early and late summer, which had been identified in former density network analyses (Björklund et al., 2017; Briffa et al., 1988, 1992). Stronger climate signals in MXD are frequently observed for seasons of two to 4 months (Esper et al., 2016) or even a single month (Edwards, Anchukaitis, et al., 2025; Torbenson et al., 2025; Trouet et al., 2018), which can, however, be more temporally unstable, as seasonal response changes over time. Overall, spatial trends of correlation strength in our data indicate a latitudinal shift southward from longer to shorter optimum target seasons for MXD calibration (Figure 4), a pattern also found in LWBI data from the Western US (Heeter et al., 2021). Among other effects (Heeter et al., 2021), this might be related to shorter growing seasons and steeper temporal gradients of solar radiation at higher latitudes (Linderholm, 2006). Thus, interannual temperature differences during spring and early summer may exert a greater influence on latewood formation in the northern half of the transect. Such conditions can be particularly impactful in the context of the complex interplay with snow melt (Kirdyanov et al., 2003; Mu et al., 2025) as well as soil thawing (Chen & Jeong, 2024), and their respective effects on tree growth. July and August are comparably crucial at the northern sites while August is clearly the most influential month for latewood formation in the south. However, a comparison of the first and second half of the investigated period (Figure S10 in Supporting Information S1) reveals that correlations with spring and early summer and thus April–September temperatures have also decreased in the north, indicating that the season used by Briffa et al. (1998) was more relevant under pre-divergence (or pre-warming) conditions than it has been since the 1960s. Meanwhile, correlations with July, August, and July–August temperatures have remained stable or even increased. The southernmost BEL site indicates the most striking example of a "midsummer decline" in correlation, as observed by Björklund et al. (2017). Although the reasons for such bimodal correlation patterns have not been conclusively identified (Maxwell et al., 2025), a simple explanation might be that midsummer temperatures in these regions are warm enough in virtually every year and do not represent a growth-limiting factor (Büntgen & Esper, 2024). Instead, heat and the resulting higher evapotranspiration may temporarily impair growth even at the upper treeline, particularly in semi-arid environments such as the Mediterranean (Römer et al., 2021) but also parts of the Western US (Elliott et al., 2020). Spatially, areas of significant correlation with temperature surrounding the nine sites encompass the entire length of the Rocky Mountains when the optimal season of highest correlation is considered and first-differencing is applied (Figure 4). Optimum seasons not only notably reduce divergence in high-frequency coherence but also in trend. Since the seasonal windows were derived from time series free of any trend after first-differencing, these improvements do not merely result from our methodology but indicate that the trends of our MXD data better match temperature trends during seasonal windows of highest sensitivity to interannual growth variability.

4.4. Regional Composites and Effects of Drought

The results for the northern part of the Rocky Mountain transect suggest that combining data into regional composites may also help mitigate non-stationarity in climate-growth relationships (Figures 6a–6f) in this region characterized by substantial spatial homogeneity in climate and tree growth patterns (Anchukaitis et al., 2013; D'Arrigo et al., 2009). Composite tree-ring and climate data may be less impacted by site-specific characteristics such as the negative outlier in MXD of 1959 at NKL, which was caused by an intense cold snap in late summer (Kunz et al., 2025; Leland et al., 2025), providing a more representative assessment of regional growth responses. Following this approach, divergence is virtually nonexistent in the north regarding both coherence and trend (Figures 6b and 6f), similar to Anchukaitis et al.'s (2013) results from the Firth River near MAC and an update from the same site based on anatomical MXD (Edwards, Anchukaitis, et al., 2025). More recent studies across NWNA have demonstrated the advantages of regional composites in combination with blue intensity data (Reid et al., 2025; Wilson et al., 2017, 2019).

The decoupling of interannual growth response and long-term trends in the south is not necessarily contradictory. While counterintuitive, it may be related to a general increase in wood density and simultaneously reduced temperature sensitivity, both caused by a larger offset between potential and actual treeline under recent warming (Büntgen et al., 2022). Droughts in the second half of the 20th century were identified as a driver of decreasing interannual temperature response of our southern sites while growth seems to have been less impaired by the "Dust Bowl" drought of the 1930s (Cook et al., 2009). Increasing aridity toward the southern edge of the Rocky Mountains (Beck et al., 2018), again in combination with the complex growth dynamics related to the regionally different upward shift of treeline and its dependence on moisture availability (Lu et al., 2025), may have weakened the relationship between MXD and temperature. This trend is particularly striking for BEL and to a lesser extent for BAK and PIK (Figure S13 in Supporting Information S1), and consistent with recent results from high-elevation pines in New Mexico (Edwards, Tintor, et al., 2025). This situation may be aggravated by an earlier loss of snowpack due to warmer spring temperatures (Hale et al., 2023; Siirila-Woodburn et al., 2021), an effect which would be most relevant for the southern sites. Although MXD is commonly considered a strong proxy for summer temperatures, drought effects on density have been observed not only at low-elevation sites, where growth is typically controlled by moisture availability (Akhmetzyanov et al., 2023), but also in generally temperature-limited sites at upper-treeline locations (De Mil et al., 2024; Römer et al., 2021; Trouet, 2014), even at high latitudes (Kunz et al., 2025). While MXD from our southern composite was strongly positively correlated with T_{max} for most of the 20th century, TRW of the same trees was negatively correlated with previous-year summer temperature throughout the entire investigated period (Figure S14b in Supporting Information S1). This relationship has become stronger in recent decades while TRW-correlations with PDSI and precipitation turned significantly positive in the 1970s, hinting at increased drought stress (Griesbauer et al., 2021). Similar observations have been made for the Pyrenees, which represent a comparable environment on the European continent (Diego Galván et al., 2015). Contradictory sensitivities of TRW and MXD to temperature and precipitation are not unheard of (Esper et al., 2020; Klippel et al., 2017). However, while the exact physiological processes contributing to MXD are still under debate (Björklund et al., 2019), insufficient water supply during early growing season, reducing photosynthesis rates and carbohydrate accumulation, may also negatively impact the density of latewood cells (Björklund et al., 2017; Kienast et al., 1987). This effect may counteract the potential of MXD to capture temperature variability in such years (Cleaveland, 1986; Yang et al., 2023). Such a reduction in signal might be amplified during longer drought periods with several consecutive years of below-average soil moisture. Growing season precipitation at our two southernmost sites is likely linked to the timing and intensity of the North American monsoon (Birch et al., 2024), which may in turn be related to ENSO (Cayan et al., 1999), further increasing the likelihood of strong precipitation anomalies and thus extensive dry spells. However, such questions regarding the interplay between functional traits, tree growth, circulation patterns, and climate response are complex (Björklund et al., 2017; Camarero, 2019) and cannot be conclusively answered with our data. However, an increasing frequency of hot droughts, represented by stronger negative correlations between T_{max} and PDSI (King et al., 2024), may further obscure interannual temperature signals, even of high-elevation sites, across this part of the WNA. In the future, such effects may become more relevant at higher latitudes under continued and accelerated warming.

5. Conclusion

We have assessed maximum latewood density (MXD) responses to temperature at nine new tree-ring sites along the Rocky Mountains and demonstrated that tree-ring records have generally continued to track instrumental temperatures despite accelerated warming across the region. This result, however, rests on highly replicated MXD data sets from near-treeline sites, application of suitable detrending methods, and consideration of site-specific seasonal temperatures. While Briffa et al.'s (1998) sampling strategy provided remarkable spatial coverage, many of their sites, particularly in NWNA, were located at elevations substantially lower than treeline, which likely weakened their temperature sensitivity. Hugershoff-detrending further limited the potential of their MXD chronologies to pick up temperature increases compared to the SF ADS detrending applied in our study. Similarly, whereas the focus on one target season (April–September) in Briffa et al. (1998) is a sensible approach to integrate different latitudes and regions across the Northern Hemisphere, it inevitably neglects the fact that the timing and length of latewood formation vary among species and sites. Correlation results, representing sensitivity to interannual temperature variability, are overall stronger in the northern half of the WNA, whereas the southern sites appear additionally affected by moisture limitations. Increasing sensitivity to hydroclimatic changes, even at high-elevation locations, will further complicate the selection of tree sites suitable for temperature reconstruction in the future. Site selection, sampling strategy, and methodological detrending and calibration choices must be considered not only in WNA but also in similar settings on different continents when evaluating divergence in tree-ring based temperature reconstructions.

Conflict of Interest

The authors declare no conflicts of interest relevant to this study.

Availability Statement

All data used for detrending, analysis, and plotting, as well as the respective R code, are archived in the OSF repository: https://doi.org/10.17605/OSF.IO/WUNMA (Kunz, 2026). This includes tree-ring data from nine sites that were sampled for this study and eight sites previously used in Briffa et al. (1998), which were downloaded from the International Tree-Ring Data Bank (ITRDB): https://www.ncei.noaa.gov/products/paleoclimatology/tree-ring. Climate data, including the Berkeley Earth (Rohde & Hausfather, 2020), CRU TS (Harris et al., 2020), and PRISM (Daly et al., 1994) products, were accessed through the KNMI Climate Explorer (Trouet & Van Oldenborgh, 2013), which was also used to produce spatial correlation maps. Raw tree-ring data were detrended using ARSTAN_49v1b (Cook, 1985; Cook et al., 2017a) and RCSSigfree_v45 (Cook et al., 2017b). The general analysis was conducted in R version 4.5.1. (R Core Team, 2024) with packages dplR (Bunn, 2008) and treeclim (Zang & Biondi, 2015). The map in Figure 1 was created using QGIS version 3.40.11 (Dawson et al., 2025).

Acknowledgments
Supported by the ERC Advanced Grant MONOSTAR (AdG 882727) and a German Science Foundation project on wood density proxies (No. 514551733). MCAT, UB, and JE received support from the ERC Synergy project SYNERGY-PLAGUE (101118880), the co-funded EU project AdAgriF (CZ.02.01.01/00/22_008/0004635), and the Czech Science Foundation Grant Hydro8 (23-08049S). EMdC received support from the German Science Foundation grant ARiD (539441548). The US National Science Foundation supported KJA and JEdw (grants AGS-2102993 and ANS-2124889), KEK (AGS-2402385), GLH (AGS-240388), and JTM (AGS-2402387). We also gratefully acknowledge the Yukon First Nations and the administration of BC Parks for granting access for sampling. We thank Sophie Spelsberg, Lisa Kinder, Julia Haber, Philipp Schulz, Daniel Bonn, Daniel Thimm, and Markus Kochbeck for their support in the field and MXD measurement. Finally, we are grateful to two anonymous reviewers whose insightful comments helped improve the manuscript.

References

Akhmetzyanov, L., Sánchez-Salguero, R., García-González, I., Domínguez-Delmás, M., & Sass-Klaassen, U. (2023). Blue is the fashion in Mediterranean pines: New drought signals from tree-ring density in southern Europe. *Science of the Total Environment*, *856*, 159291. https://doi.org/10.1016/j.scitotenv.2022.159291

Anchukaitis, K. J., D'Arrigo, R. D., Andreu-Hayles, L., Frank, D., Verstege, A., Curtis, A., et al. (2013). Tree-ring-reconstructed summer temperatures from northwestern North America during the last nine centuries. *Journal of Climate*, *26*(10), 3001–3012. https://doi.org/10.1175/JCLI-D-11-00139.1

Barber, V. A., Juday, G. P., & Finney, B. P. (2000). Reduced growth of Alaskan white spruce in the twentieth century from temperature-induced drought stress. *Nature*, *405*(6787), 668–673. https://doi.org/10.1038/35015049

Beck, H. E., Zimmermann, N. E., McVicar, T. R., Vergopolan, N., Berg, A., & Wood, E. F. (2018). Present and future Köppen-Geiger climate classification maps at 1-km resolution. *Scientific Data*, *5*(1), 180214. https://doi.org/10.1038/sdata.2018.214

Birch, J. D., DeRose, R. J., & Lutz, J. A. (2024). Spruce up your climate analysis: Dendroclimatology of Picea engelmannii and Picea pungens. *Ecosphere*, *15*(11), e70047. https://doi.org/10.1002/ecs2.70047

Björklund, J., Arx, G., Nievergelt, D., Wilson, R., van den Bulcke, J., Günther, B., et al. (2019). Scientific merits and analytical challenges of tree–ring densitometry. *Reviews of Geophysics*, *57*(4), 1224–1264. https://doi.org/10.1029/2019RG000642

Björklund, J., Seftigen, K., Kaczka, R. J., Rydval, M., & Wilson, R. (2024). A definition and standardised terminology for Blue Intensity from Conifers. https://doi.org/10.1016/j.dendro.2024.126200

Björklund, J., Seftigen, K., Schweingruber, F., Fonti, P., von Arx, G., Bryukhanova, M. V., et al. (2017). Cell size and wall dimensions drive distinct variability of earlywood and latewood density in Northern Hemisphere conifers. *New Phytologist*, *216*(3), 728–740. https://doi.org/10.1111/nph.14639

Booth, E. L. J., Byrne, J. M., & Johnson, D. L. (2012). Climatic changes in western North America, 1950–2005. *International Journal of Climatology*, *32*(15), 2283–2300. https://doi.org/10.1002/joc.3401

Bowman, D. M. J. S., Brienen, R. J. W., Gloor, E., Phillips, O. L., & Prior, L. D. (2013). Detecting trends in tree growth: Not so simple. *Trends in Plant Science*, *18*(1), 11–17. https://doi.org/10.1016/j.tplants.2012.08.005

Briffa, K. R., Jones, P. D., & Schweingruber, F. H. (1988). Summer temperature patterns over Europe: A reconstruction from 1750 A.D. based on maximum latewood density indices of conifers. *Quaternary Research*, *30*(1), 36–52. https://doi.org/10.1016/0033-5894(88)90086-5

Briffa, K. R., Jones, P. D., & Schweingruber, F. H. (1992). Tree-ring density reconstructions of summer temperature patterns across Western North America since 1600. *Journal of Climate*, *5*(7), 735–754. https://doi.org/10.1175/1520-0442(1992)005<0735:trdros>2.0.co;2

Briffa, K. R., Schweingruber, F. H., Jones, P. D., Osborn, T. J., Shiyatov, S. G., & Vaganov, E. A. (1998). Reduced sensitivity of recent tree-growth to temperature at high northern latitudes. *Nature*, *391*(6668), 678–682. https://doi.org/10.1038/35596

Bunn, A. G. (2008). A dendrochronology program library in R (dplR). *Dendrochronologia*, *26*(2), 115–124. https://doi.org/10.1016/j.dendro.2008.01.002

Büntgen, U., Allen, K., Anchukaitis, K. J., Arseneault, D., Boucher, É., Bräuning, A., et al. (2021). The influence of decision-making in tree ring-based climate reconstructions. *Nature Communications*, *12*(1), 3411. https://doi.org/10.1038/s41467-021-23627-6

Büntgen, U., & Esper, J. (2024). Physiological meaning of bimodal tree growth-climate response patterns. *International Journal of Biometeorology*, *68*(9), 1897–1902. https://doi.org/10.1007/s00484-024-02706-5

Büntgen, U., Frank, D., Wilson, R., Carrer, M., Urbinati, C., & Esper, J. (2008). Testing for tree-ring divergence in the European Alps. *Global Change Biology*, *14*(10), 2443–2453. https://doi.org/10.1111/j.1365-2486.2008.01640.x

Büntgen, U., Kirdyanov, A. V., Krusic, P. J., Shishov, V. V., & Esper, J. (2021). Arctic aerosols and the 'Divergence Problem' in dendroclimatology. *Dendrochronologia*, *67*, 125837. https://doi.org/10.1016/j.dendro.2021.125837

Büntgen, U., Piermattei, A., Crivellaro, A., Reinig, F., Krusic, P. J., Trnka, M., et al. (2022). Common Era treeline fluctuations and their implications for climate reconstructions. *Global and Planetary Change*, *219*, 103979. https://doi.org/10.1016/j.gloplacha.2022.103979

Büntgen, U., Raible, C. C., Frank, D., Helama, S., Cunningham, L., Hofer, D., et al. (2011). Causes and consequences of past and projected Scandinavian summer temperatures, 500–2100 AD. *PLoS One*, *6*(9), e25133. https://doi.org/10.1371/journal.pone.0025133

Camarero, J. J. (2019). Linking functional traits and climate-growth relationships in Mediterranean species through wood density. *IAWA Journal*, *40*(2), 215-S2. https://doi.org/10.1163/22941932-40190225

Campbell, G. G., & Vonder Haar, T. H. (1997). Comparison of surface temperature minimum and maximum and satellite measured cloudiness and radiation budget. *Journal of Geophysical Research*, *102*(D14), 16639–16645. https://doi.org/10.1029/96JD02718

Campbell, R., McCarroll, D., Loader, N. J., Grudd, H., Robertson, I., & Jalkanen, R. (2007). Blue intensity in Pinus sylvestris tree-rings: Developing a new palaeoclimate proxy. *The Holocene*, *17*(6), 821–828. https://doi.org/10.1177/0959683607080523

Cayan, D. R., Redmond, K. T., & Riddle, L. G. (1999). ENSO and hydrologic extremes in the Western United States. *Journal of Climate*, *12*(9), 2881–2893. https://doi.org/10.1175/1520-0442(1999)012<2881:eaheit>2.0.co;2

Chen, X., & Jeong, S. (2024). Asymmetric impacts of surface thaw onset change on seasonal vegetation growth in Arctic permafrost. *Global Ecology and Biogeography*, *33*(1), 131–140. https://doi.org/10.1111/geb.13769

Cleaveland, M. K. (1986). Climatic response of densitometric properties in semiarid site tree rings. Retrieved from https://repository.arizona.edu/handle/10150/261691

Cook, B. I., Miller, R. L., & Seager, R. (2009). Amplification of the North American "Dust Bowl" drought through human-induced land degradation. *Proceedings of the National Academy of Sciences*, *106*(13), 4997–5001. https://doi.org/10.1073/pnas.0810200106

Cook, E. R. (1985). *A time series analysis approach to tree ring standardization*. University of Arizona.

Cook, E. R., Briffa, K. R., Meko, D. M., Graybill, D. A., & Funkhouser, G. (1995). The "segment length curse" in long tree-ring chronology development for palaeoclimatic studies. *The Holocene*, *5*(2), 229–237. https://doi.org/10.1177/095968369500500211

Cook, E. R., & Kairiukstis, L. A. (Eds.). (1990). *Methods of dendrochronology*. Springer Netherlands. https://doi.org/10.1007/978-94-015-7879-0

Cook, E. R., Krusic, P. J., Peters, K., & Holmes, R. L. (2017a). Program ARSTAN (49v1b_MRWE), Autoregressive tree–ring standardization program.

Cook, E. R., Krusic, P. J., Peters, K., & Holmes, R. L. (2017b). Program Signal Free (version 45_ v2b), RCS Signal Free tree-ring standardization program.

CORDIS | European Commission. (n.d.). Retrieved from https://cordis.europa.eu/project/id/882727

Daly, C., Neilson, R. P., & Phillips, D. L. (1994). A statistical-topographic model for mapping climatological precipitation over mountainous terrain. *Journal of Applied Meteorology and Climatology*, *33*(2), 140–158. https://doi.org/10.1175/1520-0450(1994)033<0140:astmfm>2.0.co;2

D'Arrigo, R., Jacoby, G., Buckley, B., Sakulich, J., Frank, D., Wilson, R., et al. (2009). Tree growth and inferred temperature variability at the North American Arctic treeline. *Global and Planetary Change*, *65*(1), 71–82. https://doi.org/10.1016/j.gloplacha.2008.10.011

D'Arrigo, R., Kaufmann, R. K., Davi, N., Jacoby, G. C., Laskowski, C., Myneni, R. B., & Cherubini, P. (2004). Thresholds for warming-induced growth decline at elevational tree line in the Yukon Territory, Canada. *Global Biogeochemical Cycles*, *18*(3). https://doi.org/10.1029/2004GB002249

D'Arrigo, R., Wilson, R., Liepert, B., & Cherubini, P. (2008). On the 'Divergence Problem' in Northern Forests: A review of the tree-ring evidence and possible causes. *Global and Planetary Change*, *60*(3), 289–305. https://doi.org/10.1016/j.gloplacha.2007.03.004

Dawson, N., Fischer, J., Kuhn, M., Pasotti, A., Hugentobler, M., Rouzaud, D., et al. (2025). qgis/QGIS: 3.40.11. *Zenodo*. https://doi.org/10.5281/zenodo.17106590

De Mil, T., Matskovsky, V., Salzer, M., Corluy, L., Verschuren, L., Pearson, C., et al. (2024). Bristlecone pine maximum latewood density as a superior proxy for millennium-length temperature reconstructions. *Geophysical Research Letters*, *51*(15), e2024GL109799. https://doi.org/10.1029/2024GL109799

Diego Galván, J., Büntgen, U., Ginzler, C., Grudd, H., Gutiérrez, E., Labuhn, I., & Julio Camarero, J. (2015). Drought-induced weakening of growth–temperature associations in high-elevation Iberian pines. *Global and Planetary Change*, *124*, 95–106. https://doi.org/10.1016/j.gloplacha.2014.11.011

Edwards, J., Anchukaitis, K. J., Molina, F., Andreu-Hayles, L., D'Arrigo, R., & von Arx, G. (2025). Resolution and frequency-dependent climate signals in an arctic tree-ring temperature reconstruction of the last millennium. *Geophysical Research Letters*, *52*(20), e2025GL117846. https://doi.org/10.1029/2025GL117846

Edwards, J., Tintor, W. L., Nolin, A. F., Woodhouse, C. A., von Arx, G., & Anchukaitis, K. J. (2025). Multiple elevation-dependent climate signals from quantitative wood anatomical measurements of rocky Mountain bristlecone pine. *Journal of Geophysical Research: Biogeosciences*, *130*(1), e2024JG008307. https://doi.org/10.1029/2024JG008307

Elliott, G. P., Bailey, S. N., & Cardinal, S. J. (2020). Hotter drought as a disturbance at upper treeline in the Southern rocky Mountains. *Annals of the Association of American Geographers*, *111*(3), 756–770. https://doi.org/10.1080/24694452.2020.1805292

Esper, J., & Frank, D. (2009). Divergence pitfalls in tree-ring research. *Climatic Change*, *94*(3), 261–266. https://doi.org/10.1007/s10584-009-9594-2

Esper, J., Frank, D., Büntgen, U., Verstege, A., Hantemirov, R. M., & Kirdyanov, A. V. (2010). Trends and uncertainties in Siberian indicators of 20th century warming. *Global Change Biology*, *16*(1), 386–398. https://doi.org/10.1111/j.1365-2486.2009.01913.x

Esper, J., Frank, D. C., Wilson, R. J. S., & Briffa, K. R. (2005). Effect of scaling and regression on reconstructed temperature amplitude for the past millennium. *Geophysical Research Letters*, *32*(7). https://doi.org/10.1029/2004GL021236

Esper, J., George, S. S., Anchukaitis, K., D'Arrigo, R., Ljungqvist, F. C., Luterbacher, J., et al. (2018). Large-scale, millennial-length temperature reconstructions from tree-rings. *Dendrochronologia*, *50*, 81–90. https://doi.org/10.1016/j.dendro.2018.06.001

Esper, J., Klippel, L., Krusic, P. J., Konter, O., Raible, C. C., Xoplaki, E., et al. (2020). Eastern Mediterranean summer temperatures since 730 CE from Mt. Smolikas tree-ring densities. *Climate Dynamics*, *54*(3–4), 1367–1382. https://doi.org/10.1007/s00382-019-05063-x

Esper, J., Krusic, P. J., Ljungqvist, F. C., Luterbacher, J., Carrer, M., Cook, E., et al. (2016). Ranking of tree-ring based temperature reconstructions of the past millennium. *Quaternary Science Reviews*, *145*, 134–151. https://doi.org/10.1016/j.quascirev.2016.05.009

Esper, J., Schneider, L., Smerdon, J. E., Schöne, B. R., & Büntgen, U. (2015). Signals and memory in tree-ring width and density data. *Dendrochronologia*, *35*, 62–70. https://doi.org/10.1016/j.dendro.2015.07.001

Frank, D. C., Büntgen, U., Böhm, R., Maugeri, M., & Esper, J. (2007). Warmer early instrumental measurements versus colder reconstructed temperatures: Shooting at a moving target. *Quaternary Science Reviews*, *26*(25–28), 3298–3310. https://doi.org/10.1016/j.quascirev.2007.08.002

Frelich, L. E. (2020). Boreal and Taiga Biome. In M. I. Goldstein & D. A. DellaSala (Eds.), *Encyclopedia of the world's biomes* (pp. 103–115). Elsevier. https://doi.org/10.1016/B978-0-12-409548-9.11926-8

Fritts, H. C. (1976). *Tree rings and climate*. Elsevier Science.

Fuentes, M., Salo, R., Björklund, J., Seftigen, K., Zhang, P., Gunnarson, B., et al. (2018). A 970-year-long summer temperature reconstruction from Rogen, west-central Sweden, based on blue intensity from tree rings. *The Holocene*, *28*(2), 254–266. https://doi.org/10.1177/0959683617721322

Griesbauer, H., DeLong, S. C., Rogers, B., & Foord, V. (2021). Growth sensitivity to climate varies with soil moisture regime in spruce–fir forests in central British Columbia. *Trees*, *35*(2), 649–669. https://doi.org/10.1007/s00468-020-02066-8

Grudd, H. (2008). Torneträsk tree-ring width and density ad 500–2004: A test of climatic sensitivity and a new 1500-year reconstruction of north Fennoscandian summers. *Climate Dynamics*, *31*(7), 843–857. https://doi.org/10.1007/s00382-007-0358-2

Hale, K. E., Jennings, K. S., Musselman, K. N., Livneh, B., & Molotch, N. P. (2023). Recent decreases in snow water storage in western North America. *Communications Earth & Environment*, *4*(1), 170. https://doi.org/10.1038/s43247-023-00751-3

Harley, G. L., Heeter, K. J., Maxwell, J. T., Rayback, S. A., Maxwell, R. S., Reinemann, T. E. P., & H. Taylor, A. (2021). Towards broad-scale temperature reconstructions for Eastern North America using blue light intensity from tree rings. *International Journal of Climatology*, *41*(S1), E3142–E3159. https://doi.org/10.1002/joc.6910

Harris, I., Osborn, T. J., Jones, P., & Lister, D. (2020). Version 4 of the CRU TS monthly high-resolution gridded multivariate climate dataset. *Scientific Data*, *7*(1), 109. https://doi.org/10.1038/s41597-020-0453-3

Hartl, C., Schneider, L., Riechelmann, D. F. C., Kuhl, E., Kochbeck, M., Klippel, L., et al. (2022). The temperature sensitivity along elevational gradients is more stable in maximum latewood density than tree-ring width. *Dendrochronologia*, *73*, 125958. https://doi.org/10.1016/j.dendro.2022.125958

Heeter, K. J., Harley, G. L., Maxwell, J. T., Wilson, R. J., Abatzoglou, J. T., Rayback, S. A., et al. (2021). Summer temperature variability since 1730 CE across the low-to-mid latitudes of western North America from a tree ring blue intensity network. *Quaternary Science Reviews*, *267*, 107064. https://doi.org/10.1016/j.quascirev.2021.107064

Helama, S., Melvin, T. M., & Briffa, K. R. (2017). Regional curve standardization: State of the art. *The Holocene*, *27*(1), 172–177. https://doi.org/10.1177/0959683616652709

Holmes, R. L. (1983). Computer-assisted quality control in tree-ring dating and measurement. *Tree-Ring Bulletin*, *43*, 69–78.

Hugershoff, R. (1936). Die mathematischen Hilfsmittel der Kulturingenieurs und Biologen.

Hwangbo, N., McKinnon, K. A., & Anchukaitis, K. J. (2025). Simultaneous optimal target season estimation and local climate reconstruction using tree rings. *Geophysical Research Letters*, *52*(17), e2025GL116495. https://doi.org/10.1029/2025GL116495

IPCC. (2023). *Climate change 2021 – The Physical Science Basis: Working Group I contribution to the sixth assessment report of the intergovernmental Panel on climate change* (1st ed.). Cambridge University Press. https://doi.org/10.1017/9781009157896

Jevšenak, J., & Levanič, T. (2018). *dendroTools:* R package for studying linear and nonlinear responses between tree-rings and daily environmental data. *Dendrochronologia*, *48*, 32–39. https://doi.org/10.1016/j.dendro.2018.01.005

Kienast, F., Schweingruber, F. H., Bräker, O. U., & Schär, E. (1987). Tree-ring studies on conifers along ecological gradients and the potential of single-year analyses. *Canadian Journal of Forest Research*, *17*(7), 683–696. https://doi.org/10.1139/x87-111

King, K. E., Cook, E. R., Anchukaitis, K. J., Cook, B. I., Smerdon, J. E., Seager, R., et al. (2024). Increasing prevalence of hot drought across western North America since the 16th century. *Science Advances*, *10*(4), eadj4289. https://doi.org/10.1126/sciadv.adj4289

Kirdyanov, A. V., Arzac, A., Prokushkin, A. S., Ovchinnikov, D. V., Bondarev, A. I., Silkin, P. P., et al. (2025). Assessment of non-stationary tree growth responses in the forest-tundra and southern taiga of central Siberia. *Agricultural and Forest Meteorology*, *360*, 110296. https://doi.org/10.1016/j.agrformet.2024.110296

Kirdyanov, A. V., Hughes, M., Vaganov, E., Schweingruber, F., & Silkin, P. (2003). The importance of early summer temperature and date of snow melt for tree growth in the Siberian Subarctic. *Trees*, *17*(1), 61–69. https://doi.org/10.1007/s00468-002-0209-z

Kirdyanov, A. V., Krusic, P. J., Shishov, V. V., Vaganov, E. A., Fertikov, A. I., Myglan, V. S., et al. (2020). Ecological and conceptual consequences of Arctic pollution. *Ecology Letters*, *23*(12), 1827–1837. https://doi.org/10.1111/ele.13611

Klesse, S., DeRose, R. J., Guiterman, C. H., Lynch, A. M., O'Connor, C. D., Shaw, J. D., & Evans, M. E. K. (2018). Sampling bias overestimates climate change impacts on forest growth in the southwestern United States. *Nature Communications*, *9*(1), 5336. https://doi.org/10.1038/s41467-018-07800-y

Klippel, L., Büntgen, U., Konter, O., Kyncl, T., & Esper, J. (2020). Climate sensitivity of high- and low-elevation Larix decidua MXD chronologies from the Tatra Mountains. *Dendrochronologia*, *60*, 125674. https://doi.org/10.1016/j.dendro.2020.125674

Klippel, L., Krusic, P. J., Brandes, R., Hartl-Meier, C., Trouet, V., Meko, M., & Esper, J. (2017). High-elevation inter-site differences in Mount Smolikas tree-ring width data. *Dendrochronologia*, *44*, 164–173. https://doi.org/10.1016/j.dendro.2017.05.006

Kunz, M. (2026). Kunz_JGR_Rocky_Mountains_Divergence [Dataset]. *OSF*. https://doi.org/10.17605/OSF.IO/WUNMA

Kunz, M., Wilson, R., Reid, E., Kuhl, E., & Esper, J. (2025). Exploring potential drivers of divergence in tree-ring based temperature reconstructions of NW North America. *Dendrochronologia*, *94*, 126399. https://doi.org/10.1016/j.dendro.2025.126399

Leland, C., Davi, N., D'Arrigo, R., Andreu-Hayles, L., Pacheco-Solana, A., Edwards, J., et al. (2025). Tree-ring evidence of the elusive 1959 summer cold event in northwestern North America. *Arctic Antarctic and Alpine Research*, *57*(1), 2445945. https://doi.org/10.1080/15230430.2024.2445945

Liang, T., Tian, F., Zou, L., Gravey, M., & Rumpf, S. B. (2026). Global elevational shifts and drivers of alpine treelines. *International Journal of Applied Earth Observation and Geoinformation*, *146*, 105088. https://doi.org/10.1016/j.jag.2026.105088

Linderholm, H. W. (2006). Growing season changes in the last century. *Agricultural and Forest Meteorology*, *137*(1), 1–14. https://doi.org/10.1016/j.agrformet.2006.03.006

Loehle, C. (2009). A mathematical analysis of the divergence problem in dendroclimatology. *Climatic Change*, *94*(3), 233–245. https://doi.org/10.1007/s10584-008-9488-8

Lu, X., Zheng, X., Liang, E., Piao, S., Babst, F., Elliott, G. P., et al. (2025). Patterns, dynamics and drivers of alpine treelines and shrublines. *Nature Reviews Earth & Environment*, *6*(8), 489–502. https://doi.org/10.1038/s43017-025-00703-9

Maxwell, J. T., King, K. E., & Harley, G. L. (2025). Removing the transition wood carryover effect from latewood blue intensity to improve climate signals from *Tsuga canadensis* in the eastern United States. *Dendrochronologia*, *91*, 126344. https://doi.org/10.1016/j.dendro.2025.126344

McPartland, M. Y., St. George, S., Pederson, G. T., & Anchukaitis, K. J. (2020). Does signal-free detrending increase chronology coherence in large tree-ring networks? *Dendrochronologia*, *63*, 125755. https://doi.org/10.1016/j.dendro.2020.125755

Melvin, T. M., & Briffa, K. R. (2008). A "signal-free" approach to dendroclimatic standardisation. *Dendrochronologia*, *26*(2), 71–86. https://doi.org/10.1016/j.dendro.2007.12.001

Melvin, T. M., Briffa, K. R., Nicolussi, K., & Grabner, M. (2007). Time-varying-response smoothing. *Dendrochronologia*, *25*(1), 65–69. https://doi.org/10.1016/j.dendro.2007.01.004

Mu, Y.-Q., Che, T., Dai, L.-Y., Liu, S.-W., & Wang, G.-G. (2025). Interplay between snow phenology and vegetation phenology in Alaska under climate change. *Advances in Climate Change Research*, *16*(3), 490–500. https://doi.org/10.1016/j.accre.2025.04.001

Nehrbass-Ahles, C., Babst, F., Klesse, S., Nötzli, M., Bouriaud, O., Neukom, R., et al. (2014). The influence of sampling design on tree-ring-based quantification of forest growth. *Global Change Biology*, *20*(9), 2867–2885. https://doi.org/10.1111/gcb.12599

Pearl, J. K., Anchukaitis, K. J., Pederson, N., & Donnelly, J. P. (2017). Reconstructing Northeastern United States temperatures using Atlantic white cedar tree rings. *Environmental Research Letters*, *12*(11), 114012. https://doi.org/10.1088/1748-9326/aa8f1b

Perkins-Kirkpatrick, S. E., & Lewis, S. C. (2020). Increasing trends in regional heatwaves. *Nature Communications*, *11*(1), 3357. https://doi.org/10.1038/s41467-020-16970-7

Piechota, T., Timilsena, J., Tootle, G., & Hidalgo, H. (2004). The western U.S. drought: How bad is it? *EOS Transactions of the American Geophysical Union*, *85*(32), 301–304. https://doi.org/10.1029/2004EO320001

Porter, T. J., & Pisaric, M. F. J. (2011). Temperature-growth divergence in white spruce forests of Old Crow Flats, Yukon Territory, and adjacent regions of northwestern North America. *Global Change Biology*, *17*(11), 3418–3430. https://doi.org/10.1111/j.1365-2486.2011.02507.x

Portmann, R. W., Solomon, S., & Hegerl, G. C. (2009). Spatial and seasonal patterns in climate change, temperatures, and precipitation across the United States. *Proceedings of the National Academy of Sciences*, *106*(18), 7324–7329. https://doi.org/10.1073/pnas.0808533106

R Core Team. (2024). *R: A language and environment for statistical computing*. R Foundation for Statistical Computing.

Reid, E., Luckman, B., Kunz, M., Esper, J., D'Arrigo, R., Leland, C., & Wilson, R. (2025). Expanding the Yukon tree ring Blue Intensity network to assess divergence effects and enhance climate reconstructions. *The Holocene*.

Rinn, F. (2003). TSAP-Win™. Retrieved from http://www.rinntech.de/content/view/17/48/lang,german/index.html

Rohde, R., & Hausfather, Z. (2020). The Berkeley Earth Land/Ocean temperature record. *Earth System Science Data*, *12*(4), 3469–3479. https://doi.org/10.5194/essd-12-3469-2020

Rohde, R., Muller, R., Jacobsen, R., Perlmutter, S., & Mosher, S. (2013). Berkeley Earth temperature averaging process. *Geoinformatics & Geostatistics: An Overview*, *1*(2). https://doi.org/10.4172/2327-4581.1000103

Römer, P., Hartl, C., Schneider, L., Bräuning, A., Szymczak, S., Huneau, F., et al. (2021). Reduced temperature sensitivity of maximum latewood density formation in high-elevation Corsican pines under recent warming. *Atmosphere*, *12*(7), 804. https://doi.org/10.3390/atmos12070804

Rydval, M., Larsson, L.-Å., McGlynn, L., Gunnarson, B. E., Loader, N. J., Young, G. H. F., & Wilson, R. (2014). Blue intensity for dendroclimatology: Should we have the blues? Experiments from Scotland. *Dendrochronologia*, *32*(3), 191–204. https://doi.org/10.1016/j.dendro.2014.04.003

Salzer, M. W., Hughes, M. K., Bunn, A. G., & Kipfmueller, K. F. (2009). Recent unprecedented tree-ring growth in bristlecone pine at the highest elevations and possible causes. *Proceedings of the National Academy of Sciences*, *106*(48), 20348–20353. https://doi.org/10.1073/pnas.0903029106

Schweingruber, F. H., & Briffa, K. R. (1996). Tree-ring density networks for climate reconstruction. In P. D. Jones, R. S. Bradley, & J. Jouzel (Eds.), *Climatic variations and forcing mechanisms of the last 2000 years* (pp. 43–66). Springer. https://doi.org/10.1007/978-3-642-61113-1_3

Seftigen, K., Fonti, M. V., Luckman, B., Rydval, M., Stridbeck, P., von Arx, G., et al. (2022). Prospects for dendroanatomy in paleoclimatology – A case study on *Picea engelmannii* from the Canadian Rockies. *Climate of the Past*, *18*(5), 1151–1168. https://doi.org/10.5194/cp-18-1151-2022

Siirila-Woodburn, E. R., Rhoades, A. M., Hatchett, B. J., Huning, L. S., Szinai, J., Tague, C., et al. (2021). A low-to-no snow future and its impacts on water resources in the western United States. *Nature Reviews Earth & Environment*, *2*(11), 800–819. https://doi.org/10.1038/s43017-021-00219-y

Stage, A. R. (1976). An expression for the effect of aspect, slope, and habitat type on tree growth. *Forest Science*, *22*(4), 457–460. https://doi.org/10.1093/forestscience/22.4.457

Stanhill, G., & Cohen, S. (2001). Global dimming: A review of the evidence for a widespread and significant reduction in global radiation with discussion of its probable causes and possible agricultural consequences. *Agricultural and Forest Meteorology*, *107*(4), 255–278. https://doi.org/10.1016/S0168-1923(00)00241-0

Stine, A. R., & Huybers, P. (2014). Arctic tree rings as recorders of variations in light availability. *Nature Communications*, *5*(1), 3836. https://doi.org/10.1038/ncomms4836

Sullivan, P. F., Pattison, R. R., Brownlee, A. H., Cahoon, S. M. P., & Hollingsworth, T. N. (2016). Effect of tree-ring detrending method on apparent growth trends of black and white spruce in interior Alaska. *Environmental Research Letters*, *11*(11), 114007. https://doi.org/10.1088/1748-9326/11/11/114007

Torbenson, M. C. A., Martinez Del Castillo, E., Reinig, F., Stahle, D. W., King, K. E., Maxwell, J. T., et al. (2025). Lack of cold temperatures is driving recent high-summer warming in the southern Rocky Mountains. *International Journal of Biometeorology*, *69*(6), 1475–1486. https://doi.org/10.1007/s00484-025-02904-9

Trenberth, K. E., Branstator, G. W., & Arkin, P. A. (1988). Origins of the 1988 North American Drought. *Science*, *242*(4886), 1640–1645. https://doi.org/10.1126/science.242.4886.1640

Trouet, V. (2014). A tree-ring based late summer temperature reconstruction (AD 1675–1980) for the Northeastern mediterranean. *Radiocarbon*, *56*(4), S69–S78. https://doi.org/10.2458/azu_rc.56.18323

Trouet, V., Babst, F., & Meko, M. (2018). Recent enhanced high-summer North Atlantic Jet variability emerges from three-century context. *Nature Communications*, *9*(1), 180. https://doi.org/10.1038/s41467-017-02699-3

Trouet, V., & Van Oldenborgh, G. J. (2013). KNMI climate explorer: A web-based research tool for high-resolution paleoclimatology. *Tree-Ring Research*, *69*(1), 3–13. https://doi.org/10.3959/1536-1098-69.1.3

Vaganov, E. A., Hughes, M. K., & Shashkin, A. V. (2011). *Growth dynamics of conifer tree rings: Images of past and future environments*. Springer.

Wang, X., Zhang, M., Ji, Y., Li, Z., Li, M., & Zhang, Y. (2017). Temperature signals in tree-ring width and divergent growth of Korean pine response to recent climate warming in northeast Asia. *Trees*, *31*(2), 415–427. https://doi.org/10.1007/s00468-015-1341-x

Wells, N., Goddard, S., & Hayes, M. J. (2004). A self-calibrating palmer drought severity index. *Journal of Climate*, *17*(12), 2335–2351. https://doi.org/10.1175/1520-0442(2004)017<2335:aspdsi>2.0.co;2

Wigley, T. M. L., Briffa, K. R., & Jones, P. D. (1984). On the average value of correlated time series, with applications in dendroclimatology and hydrometeorology. *Journal of Applied Meteorology and Climatology*, *23*(2), 201–213. https://doi.org/10.1175/1520-0450(1984)023<0201:otavoc>2.0.co;2

Wild, M. (2009). Global dimming and brightening: A review. *Journal of Geophysical Research*, *114*(D10). https://doi.org/10.1029/2008JD011470

Wilson, R., Anchukaitis, K., Andreu-Hayles, L., Cook, E., D'Arrigo, R., Davi, N., et al. (2019). Improved dendroclimatic calibration using blue intensity in the southern Yukon. *The Holocene*, *29*(11), 1817–1830. https://doi.org/10.1177/0959683619862037

Wilson, R., Anchukaitis, K., Briffa, K. R., Büntgen, U., Cook, E., D'Arrigo, R., et al. (2016). Last millennium northern hemisphere summer temperatures from tree rings: Part I: The long term context. *Quaternary Science Reviews*, *134*, 1–18. https://doi.org/10.1016/j.quascirev.2015.12.005

Wilson, R., D'Arrigo, R., Andreu-Hayles, L., Oelkers, R., Wiles, G., Anchukaitis, K., & Davi, N. (2017). Experiments based on blue intensity for reconstructing North Pacific temperatures along the Gulf of Alaska. *Climate of the Past*, *13*(8), 1007–1022. https://doi.org/10.5194/cp-13-1007-2017

Wilson, R., & Luckman, B. H. (2003). Dendroclimatic reconstruction of maximum summer temperatures from upper treeline sites in Interior British Columbia, Canada. *The Holocene*, *13*(6), 851–861. https://doi.org/10.1191/0959683603hl663rp

Wilson, R., Rao, R., Rydval, M., Wood, C., Larsson, L.-Å., & Luckman, B. H. (2014). Blue Intensity for dendroclimatology: The BC blues: A case study from British Columbia, Canada. *The Holocene*, *24*(11), 1428–1438. https://doi.org/10.1177/0959683614544051

Yang, B., He, M., Yang, L., Wang, F., & Ljungqvist, F. C. (2023). Pine maximum latewood density in semi-arid northern China records hydroclimate rather than temperature. *Geophysical Research Letters*, *50*(13), e2023GL104362. https://doi.org/10.1029/2023GL104362

Zang, C., & Biondi, F. (2015). treeclim: An R package for the numerical calibration of proxy-climate relationships. *Ecography*, *38*(4), 431–436. https://doi.org/10.1111/ecog.01335